Atmos. Chem. Phys. Discuss., 9, 9793–9822, 2009
www.atmos-chem-phys-discuss.net/9/9793/2009/

Atmospheric Chemistry and Physics Discussions

This discussion paper is/has been under review for the journal *Atmospheric Chemistry and Physics (ACP)*. Please refer to the corresponding final paper in *ACP* if available.

Carbon monoxide distributions from the IASI/METOP mission: evaluation with other space-borne remote sensors

M. George[1], C. Clerbaux[1], D. Hurtmans[2], S. Turquety[1,*], P.-F. Coheur[2], M. Pommier[1], J. Hadji-Lazaro[1], D. P. Edwards[3], H. Worden[3], M. Luo[4], C. Rinsland[5], and W. McMillan[6]

[1]UPMC Université Paris 06, CNRS UMR8190, LATMOS/IPSL, France
[2]Spectroscopie de l'Atmosphère, Service de Chimie Quantique et Photophysique, Université Libre de Bruxelles (ULB), Brussels, Belgium
[3]Atmospheric Chemistry Division, National Center for Atmospheric Research, Boulder, Colorado, USA
[4]Jet Propulsion Laboratory, California Institute of Technology, Pasadena, California, USA
[5]NASA Langley Research Center, Hampton, Virginia, USA

[6] Center for Satellite Applications and Research, National Environmental Satellite, Data and Information Service, NOAA, Camp Springs, Maryland, USA
[*] now at: UPMC Université Paris 06, Laboratoire de Météorologie Dynamique/IPSL, Ecole Polytechnique, Palaiseau, France

Received: 24 February 2009 – Accepted: 13 March 2009 – Published: 17 April 2009

Correspondence to: M. George (maya.george@latmos.ipsl.fr)

Published by Copernicus Publications on behalf of the European Geosciences Union.

Abstract

The Infrared Atmospheric Sounding Interferometer (IASI) onboard the MetOp satellite measures carbon monoxide (CO) on a global scale, twice a day. CO total columns and vertical profiles are retrieved in near real time from the nadir radiance spectra measured by the instrument in the thermal infrared (TIR) spectral range. This paper describes the measurement vertical sensitivity of IASI. On the global scale, 0.8 to 2.4 independent pieces of information are available for the retrieval. At mid latitudes, the information ranges between 1.5 and 2, which enables the lower and upper troposphere to be distinguished, especially when thermal contrast is important. Global distributions of column CO are evaluated with correlative observations available from other nadir looking TIR missions currently in operation: the Measurements of Pollution in the Troposphere (MOPITT) onboard TERRA, the Atmospheric Infrared Sounder (AIRS) onboard AQUA and the Tropospheric Emission Spectrometer (TES) onboard AURA. On the global scale and on average, total column discrepancies ranging from 10 to 15% are found for latitudes above 45° N and lower than 15° S, but can reach 30% in cases of strong CO concentrations, e.g. when fires events occur. The choice of the a priori assumptions influences the retrievals and can explain some of the observed differences. Instrument specifications of IASI versus other missions are also discussed.

1 Introduction

As one of the most important precursors of O_3, carbon monoxide (CO) is an important trace gas for the understanding of both air quality and climate forcing. Formed by the incomplete combustion of fossil and bio-fuels, and by vegetation burning, CO is also produced in the atmosphere via the oxidation of methane and non-methane hydrocarbons by the hydroxyl radical (OH) (Duncan et al., 2008). It is the largest global sink of the OH radical and thus plays an important role in the oxidizing power of the atmo-

ACPD

9, 9793–9822, 2009

sphere and in the concentrations of greenhouses gases such as CH_4 and O_3. Because of its relatively long lifetime (a few weeks to a few months depending on latitude and time of year), CO has been extensively used as an atmospheric tracer of transport (Logan et al., 1981).

CO is routinely measured by ground-station networks (Kurylo, 1991; Pougachev and Rinsland, 1995; Novelli et al., 1998; Yurganov et al., 2004, 2005; Velazco et al., 2007; Zander et al., 2008), airborne measurements campaigns, airborne networks (Nedelec et al., 2005) and by instruments onboard satellites. In recent years, extensive CO observations from space, from a number of satellite platforms have yielded a global view of the CO distribution, from the troposphere to the mesosphere. Limb-sounders (in absorption or emission) can derive vertically resolved profiles for the mid/high-troposphere and upper, with a limited spatial coverage (e.g. SMR/ODIN (Barret et al., 2006), MIPAS/ENVISAT (Funke et al., 2007), MLS/AURA, Pumphrey et al., 2007; Livesey et al., 2008, and ACE-FTS/SCISAT-1, Clerbaux et al., 2008a). Nadir viewing remote sensors offer the advantage of sounding into the lower atmosphere, although with a limited vertical resolution, as was demonstrated from MOPITT/TERRA (Deeter et al., 2003; Edwards et al., 2004), SCIAMACHY (Frankenberg et al., 2005; Buchwitz et al., 2007), TES/AURA (Rinsland et al., 2006; Luo et al., 2007a and b), AIRS/AQUA (McMillan et al., 2005), and IASI/MetOp (Turquety et al., 2004; Clerbaux et al., 2009). Both nadir viewing and limb viewing instruments are often impacted by the presence of clouds. Time series of CO measurements show the impact of inter-annual variations, for example a moderate El Niño event in 2006 (Rinsland et al., 2008).

Validation of satellite CO retrievals with space-borne, air-borne or ground-based measurements has already been performed in the frame of different exercises or campaigns (Clerbaux et al., 2002, 2008a; Emmons et al., 2004, 2007, 2009; Warner et al., 2007; Luo et al., 2007a, b; Yurganov et al., 2008). In this paper, we focus on the analysis of global CO distributions recently calculated from the radiance spectra recorded by the IASI instrument. A case study of the Mediterranean fires during the summer of 2007, which illustrates the capability of IASI to measure extreme CO concentrations and to track the plume from wildfires is presented in a companion paper (Turquety et al., 2009). Here we compare the IASI global distributions with CO observations available from other operational nadir looking instruments which also record surface and atmospheric signals in the thermal infrared (TIR) spectral range: MOPITT, AIRS and TES. This paper presents a preliminary and non exhaustive validation overview rather than a quantitative comparison of the IASI CO retrievals obtained by the Fast Operational/Optimal Retrievals on Layers for IASI (FORLI) algorithm, developed at ULB and based on the optimal estimation method which is thoroughly described by Turquety et al. (2009). In the first global validation of these products, for simplicity, we compare total column CO results.

The paper is organized as follows: First we describe the IASI-CO measurements as routinely retrieved from the operational EUMETSAT radiance products. Next we compare the CO total column distributions retrieved by MOPITT, AIRS and TES data for the August 2008 period. And finally we conclude with an analysis of the observed agreement and discrepancy.

2 IASI: CO column and profile retrievals

2.1 The IASI mission

The polar-orbiting MetOp-A, launched on 19 October 2006 is the first of three successive MetOp satellites. As a component of the space segment of the EUMETSAT Polar System (EPS), this operational meteorological platform carries the Infrared Atmospheric Sounding Interferometer (IASI), a nadir-looking high resolution Fourier Transform Spectrometer (FTS). IASI is designed to provide atmospheric temperature and water vapour profiles for operational meteorology. Thanks to its apodized spectral resolution of 0.5 cm^{-1} (with a spectral sampling of 0.25 cm^{-1}), its large spectral range (from 645 to 2760 cm^{-1} with no gaps), and its low radiometric noise (from on-flight analysis the Noise Equivalent Delta Temperature (NEDT) is estimated to range from 0.1–0.4 K, Clerbaux et al., 2009), atmospheric concentrations for several key species important to climate forcing and atmospheric chemistry monitoring can be derived from IASI radiance measurements. Such species include not only the predominant CO (Turquety et al., 2009), O_3 (Boynard et al., 2009), CH_4 (Razavi et al., 2009), HNO_3 (Wespes et al., 2009) molecules but also weak absorbing molecules detected during extraordinary events, such as SO_2 during volcanic eruption (Clarisse et al., 2008) or reactive species in fire plumes (Coheur et al., 2009). In addition, IASI offers an excellent horizontal coverage due to its across track swath width of 2200 km, allowing global coverage twice a day, with a field of view sampled by 2×2 circular pixels each with a 12 km footprint diameter.

2.2 CO measurements

CO distributions are retrieved from IASI radiance spectra using the FORLI-CO software. Based on the Optimal Estimation Method (OEM) described by Rodgers (2000), this algorithm is described in detail in Turquety et al. (2009). The a priori mean profile and associated variability matrix were constructed using a database of observations that included aircraft profiles from the MOZAIC (Measurement of OZone and water vapour by AIrbus in-service air-Craft) program (Nedelec et al., 2003), and ACE-FTS satellite observations in the upper troposphere and above (Clerbaux et al., 2005). These were complemented with distributions from the LMDz-INCA global model (Turquety et al., 2008) in order to build a matrix representative of both background and polluted conditions. IASI Level 1C radiance data are analysed in near real time (observation+∼3 h) and for the study presented here, only cloud free data are analysed. The code uses the water vapour and temperature profiles from IASI Level 2 data and operationally distributed by EUMETSAT through the EUMETCAST dissemination system (Schluessel et al., 2005) as input variables. FORLI-CO provides CO profiles for at most 19 layers (from the surface to the top of the atmosphere), as well as error and characterization diagnostics, in particular an a posteriori error variance-covariance matrix and an averaging kernel matrix. Figure 1 illustrates, in equivalent

ACPD

9, 9793–9822, 2009

brightness temperatures, the IASI spectral range that is used for the CO retrieval ($2143–2181.25\,cm^{-1}$). It was chosen in order to avoid most of the other absorbing species in the CO spectral range (i.e. H_2O, O_3, CO_2 and N_2O). The plot also shows the (observed-calculated) residual after the retrieval for a typical observation (located over the West coast of the USA), which could be directly compared with the IASI radiometric noise level.

Averaging kernels (also see Fig. 1) characterize the sensitivity of each measurement to the true CO profile, with the remainder of the information provided by the a priori profile:

$$\hat{\mathbf{x}} = \mathbf{A}\mathbf{x} + (\mathbf{I} - \mathbf{A})\,\mathbf{x}_a \quad (1)$$

with $\hat{\mathbf{x}}$ the retrieved profile, $\mathbf{A}$ the averaging kernel matrix, $\mathbf{x}$ the true profile and $\mathbf{x}_a$ the a priori profile.

The rows of the averaging kernel matrix describe the change to the retrieval state at a specific altitude to a perturbation of the true state vector and provide an estimation of the vertical resolution (full width at half maximum). The trace of the matrix, known as the degrees of freedom for signal (DOFS), is a metric used to measure the number of independent pieces of information available from the retrieval (Rodgers, 2000). In the example presented in Fig. 1, the set of averaging kernels presents two maxima (at the surface and around 6 km) and the DOFS number is 2.14.

As described in previous papers (e.g. Deeter et al., 2007; Clerbaux et al., 2008b, 2009) the thermal contrast (i.e. the temperature difference between the surface and the first atmospheric layer) is a critical parameter for the understanding of the vertical information contained in the CO product. For the example described here, the measurement is performed at a location associated with a large thermal contrast (close to Los Angeles, USA, morning orbit) and hence the averaging kernels corresponding to the lower layers exhibit large sensitivity at the surface. Two independent partial columns can be retrieved, allowing the separation of the CO concentration in the boundary layer from the mid troposphere. In contrast, for other atmospheric conditions

ACPD
9, 9793–9822, 2009

(e.g. see Fig. 4), where the thermal contrast is less favourable, there is no sensitivity at the surface.

Figure 2 illustrates one day (1 August 2008) of IASI CO observations, both for day and night measurements, along with the corresponding surface temperature from IASI Level 2 data, thermal contrast (as calculated from the difference between surface temperature and the temperature of the first available atmospheric level), and DOFS. As expected, differences appear between day and night distributions, which can be linked directly to the thermal contrast, which is much more pronounced during the day than during the night. This reflects onto the DOFS numbers that are larger over areas where the thermal contrast exceeds a few degrees. On the global scale, DOFS values range between 0.8 and 2.4, for this specific day. These values are also representative for other time periods. Generally, for latitudes above and below 60° only a total column (DOFS around 1) could be retrieved. At mid latitudes, the information ranges between 1.5 and 2, allowing the lower and upper troposphere to be distinguished. For very cold areas, e.g. Antarctic during the night, the retrieval profile consists merely in the a priori profile. On the contrary, for hot locations during the day, the DOFS can provide two pieces of independent information and the retrievals are much less weighted by the a priori.

3 CO correlative measurements distribution

In order to compare the FORLI-CO results we use similar products available from other currently operational nadir looking TIR instruments: MOPITT, AIRS and TES. In the following sections, we present briefly the retrieval methods and the a priori of each instrument. The choice of the a priori is crucial for the inversion as shown in Luo et al. (2007a), especially for down-looking spectrometers which lack measurement sensitivity in the lower atmosphere. We then focus on monthly averaged total column CO distributions for August 2008 to derive general trends in terms of discrepancies. A general description of the different missions and instrument specifications is provided in

ACPD
9, 9793–9822, 2009

Table 1.

3.1 Retrieval methods and a priori

3.1.1 MOPITT

MOPITT uses correlation radiometry (Drummond, 1989) and the terrestrial thermal emission to sound tropospheric CO. More recently, it was also shown that the solar channels provide supplementary information (Deeter et al., 2009). CO retrievals are obtained by using a maximum a posteriori method that incorporates a priori information of the physical and statistical variability of the trace gas distribution in the atmosphere (Pan et al., 1998). For this study we use MOPITT V3 data which are filtered for clouds. This version uses a single CO a priori profile and the covariance matrix is derived from several hundred in situ CO data distributed globally (Deeter et al., 2003). We note that a MOPITT V4 product will be available soon, with improvements such as log-normal statistics for VMR, a modified forward model that handles extreme pollution conditions, and variable a priori profiles. Differences between the global a priori profile used in V3 and the geographically and temporally variable a priori profiles used in V4 might lead to significant differences in CO total column values.

3.1.2 TES

TES nadir Global Survey (GS) observations consist of 16 orbits in a 26 h period; a new GS starts every other day. The along orbit observations are made approximately every 180 km. The TES CO prior information is derived from a year of simulation with the MOZART model (Brasseur et al., 1998). The prior profiles are monthly means in blocks of $10^{\circ} \times 60^{\circ}$ (latitude by longitude). TES CO retrievals apply modified Tikhanov constraints (Kulawik et al., 2008). Spectral micro windows with isolated CO lines are used in CO retrievals (Rinsland et al., 2006). Here we use TES V004 GS data. Data quality and cloud filtering criteria are used to select TES CO total columns according

ACPD

9, 9793–9822, 2009

Carbon monoxide distributions from the IASI/METOP mission

M. George et al.

to TES Level 2 Data User's Guide (Osterman et al., 2008).

3.1.3 AIRS

Tropospheric CO abundances are retrieved from AIRS cloud-cleared radiances, utilizing a set of overlapping trapezoidal perturbation functions, similar to the retrieval of all AIRS products (Susskind et al., 2003). Version 5 (V5) AIRS CO retrievals used in this analysis differ from the V4 products used in previous studies (McMillan et al., 2005, 2008; Warner et al., 2007; Yurganov et al., 2008) in terms of the number of trapezoidal functions and the first guess profile. V5 employs the MOPITT V3 a priori profile as a single global first guess profile with nine trapezoidal perturbation functions (Comer, 2006). The lowest of these nine functions were chosen to closely coincide with the seven reporting levels for MOPITT CO retrievals. Overall, the nine functions better define the shape of the AIRS CO averaging kernels versus the V4 four trapezoidal functions described in McMillan et al. (2008). The nine functions represent coarse supersets of the AIRS 100 layer radiative transfer model. At most DOFS numbers are 1.5 in AIRS CO retrievals, but typical values are closer to 0.8. For this study, AIRS V5 data were accessed through the NASA Goddard DAAC and filtered with quality indicators as suggested in the AIRS Version 5 Level-2 Standard Product Quickstart guide.

3.2 Spectral resolution and vertical sensitivity

Spectra recorded by the three spectrometer type instruments IASI, TES and AIRS above the same area are presented in Fig. 3, for the full spectral range covered by each (see Table 1). The data correspond to nadir along track observations only (North Brazil), which explains the relative poor coincidence criteria, and the time of recording differs by a few hours at maximum. From these plots the TES higher spectral resolution is well marked, as are the advantages of AIRS in terms of signal to noise ratio and of IASI in terms of spectral coverage. As MOPITT is a gas correlation radiometer, the radiance signal is not directly comparable.

ACPD

9, 9793–9822, 2009

Carbon monoxide distributions from the IASI/METOP mission

M. George et al.

Figure 4 illustrates the averaging kernel functions of IASI, MOPITT, AIRS and TES for the same coincident observation. The functions have similar shapes, with low sensitivity near the surface and maximum sensitivity in the low troposphere (4–6 km), which highlight more the dependencies of the infrared nadir observation to the geophysical scene rather than to the instrument performance. The number of levels retrieved differs markedly for each instrument (IASI=19, MOPITT=7, AIRS=9, TES=67) and is not representative of the vertical resolution. This also explains the different absolute values of the averaging kernels, with higher peak values for thicker layers. For IASI, MOPITT and TES, the numbers of DOFS are larger than 1, illustrating that the information of the total column comes from more than one layer of the atmosphere. The low AIRS DOFS number for this retrieval likely results from partially cloudy scenes. The low sensitivity to the surface can be mostly explained by the lack of thermal contrast for this scene above an area of forest. However the comparison of such averaging kernel functions and DOFS numbers is indicative but not quantitative as the a priori and the retrieval methods are different.

3.3 Comparison of CO total column for August 2008

In the following we focus on monthly averaged total column CO distributions to derive general trends in terms of discrepancies. Figure 5 presents CO total columns retrieved from IASI, MOPITT, AIRS and TES data available for August 2008. The study focuses on August because it is an interesting period to observe high CO concentrations in Africa due to intensive agriculture fires. Other periods/seasons have also been examined and it was found that the same conclusion holds. We have decided to compare data averaged over a month and over a 1°×1°grid to lower the differences associated with the different temporal and spatial ranges of each satellite. Only daytime observations are shown here. The different a priori assumptions – CO covariance as well as the a priori profile – are expected to make a significant difference (Luo et al., 2007a) and can also change the apparent DOFS.

A good agreement is found between the four distributions, with CO total column values ranging from 4×10^{17} molecules/cm^2 (background level) to more than 4×10^{18} molecules/cm^2 (fire events), though the IASI background data are lower than those associated with the other distributions. The largest concentrations are observed by all four instruments, although with different intensity, over China (pollution), Africa and South America (vegetation fires). IASI and MOPITT distributions show very similar intensities for the African fires. IASI and AIRS have some problems with the inversion of spectra recorded above deserts in North Africa or in the Arabic Peninsula: high concentrations are visible for IASI and the data were filtered for AIRS (in light grey, bottom left plot in Fig. 5). IASI and AIRS results have the best horizontal coverage.

Figure 6 shows scatter plots of the averaged CO total columns (1°×1° gridded) for IASI as compared to MOPITT, AIRS and TES, for different latitude bands (Global i.e. [−90°; 90], [45°; 90°], [15°; 45°], [−15°; 15°] and [−45°; −15°]). Also shown are the histograms of the relative differences in percent (200×(IASI-INSTR)/(IASI+INSTR), with INSTR=MOPITT, AIRS or TES) averaged the same way. Table 2 provides the corresponding correlation coefficients, as well as the slope and intercept of the linear regression line. The correlation is generally good, although some biases are observed. For data averaged over all latitudes (Fig. 6a, f, and k), the coefficients are 0.82 (IASI/MOPITT), 0.91 (IASI/AIRS) and 0.83 (IASI/TES). This indicates that the four instruments can capture the dynamic range of the CO concentration with a good agreement. In the equatorial region (latitudes [−15; 15°], Fig. 6d, i and n) MOPITT, AIRS and TES are very well correlated with IASI, with correlation coefficients of 0.93, 0.94 and 0.87, respectively. However MOPITT is consistently higher than IASI with an average bias of 12% for data averaged over all latitudes (Fig. 6p) (10.1% for latitudes [45°; 90°] (Fig. 6q) and 16.6% for latitudes [−4°; −15°], Fig. 6t). This is consistent with a positive bias reported for MOPITT (V3 data) as shown in Emmons et al. (2009). AIRS also shows a important bias for the southern latitudes: 15.6% higher than IASI between 15° S and 45° S (Fig. 6t) but is in close agreement with IASI between 15° N and 45° N (Fig. 6g and q). In other regions, AIRS CO data seems to be larger than IASI for weak concentrations but lower for high concentrations (Fig. 6f, g, h, i and j) indicating a more restricted dynamic range for AIRS retrievals due to the lower DOFS for AIRS CO as has been previously noted (Warner et al., 2007; Yurganov et al., 2008). On the contrary, TES is lower than IASI in all the latitude regions (8.7%, Fig. 6p).

4 Summary and conclusions

This paper presents a first assessment of the capabilities of IASI to measure CO on the global scale. The results presented here were obtained with the FORLI-CO algorithm, a near real time processing code that delivers atmospheric profiles of CO about three hours after the observation. Several months of observations have been analyzed, and both total column and coarse vertical profiles have been measured on the global scale, twice a day. CO quick-look distributions maps with different projections can be viewed from the LATMOS website at http://iasi-chem.aero.jussieu.fr. The vertical information available is strongly dependent on ground temperature and thermal contrast, with the daytime data being more useful for studying the atmospheric composition in the lowest parts of the atmosphere. Sensitivity at the surface level varies as a function of thermal contrast and local emissivity. Several radiative transfer issues remain when processing the IASI data over very cold/icy and very hot/sandy surfaces, for which we lack correct emissivity data, which is not yet available from EUMETCAST.

This paper provides a preliminary assessment of the IASI CO global distributions by comparing the product obtained by FORLI-CO with that provided by other space-borne instruments that also exploit the thermal infrared spectral range to sound the atmosphere. In the Northern Hemisphere and in the equatorial region, the comparison presented here for August 2008 shows an agreement better than ∼11% between IASI and the three other IR sounders. In the Southern Hemisphere, under 15° S, IASI is about 15% lower on average than MOPITT and AIRS. For large concentrations of CO, such as in fires events, IASI and MOPITT are in good agreement, but AIRS is systematically lower than IASI (30%), likely due to the combination of AIRS coarser spectral resolution and larger retrieval footprint (45 km). TES shows a similar distribution struc-

ACPD
9, 9793–9822, 2009

ture but is consistantly lower than IASI, for all latitudes bands. Column comparisons could still be biased by different a priori used by the retrievals. Further studies are needed to improve first guess a priori profiles, climatologies, statistics, and ancillary data. Profile comparisons (with in situ observations, as they become available for the IASI time period: POLARCAT campaign, MOZAIC network) will account for averaging kernel and a priori differences. There is also a need to provide better knowledge of the Earth's surface temperature, atmospheric temperature and humidity profiles. Such improvements would improve the accuracy of CO satellite remote sensing retrievals, especially for nadir viewing thermal sounding instruments such as TES, AIRS, MOPITT and IASI.

Acknowledgements. IASI has been developed and built under the responsibility of the Centre National d'Etudes Spatiales (CNES, France). It is flown onboard the MetOp satellites as part of the EUMETSAT Polar System. The IASI L1 data are received through the EUMETCAST near real time data distribution service. IASI L1 and L2 data are stored in the Ether French atmospheric database (http://ether.ipsl.jussieu.fr). The research in France is conducted with the financial support of CNES. The research in Belgium was funded by the "Actions de Recherche Concertées" (Communauté Française), the Fonds National de la Recherche Scientifique (FRS-FNRS F.4511.08), the Belgian State Federal Office for Scientific, Technical and Cultural Affairs and the European Space Agency (ESA-Prodex C90-327). The authors are grateful to INSU for publication support. Analysis of TES measurements at NASA Langley Research Center is supported by NASA's Upper Atmospheric Chemistry and Modeling Program (ACMAP) and Upper Atmosphere Research Program (UARP). Analysis of AIRS CO retrievals is supported by the AIRS Project (JPL) and NASA's Tropospheric Chemistry Program.

The publication of this article is financed by CNRS-INSU.

References

Aumann, H. H., Chahine, M. T., Gautier, C., Goldberg, M. D., Kalnay, E., McMillin, L. M., Revercomb, H., Rosenkranz, P. W., Smith, W. L., Staelin, D. H., Strow, L. L., and Susskind, J.: AIRS/AMSU/HSB on the Aqua mission: Design, science objectives, data products, and processing systems, IEEE T. Geosci. Remote, 41(2), 253–264, 2003.

Barret, B., Ricaud, P., Santee, M. L., Attie, J.-L., Urban, J., Le Flochmoen, E., Berthet, G., Murtagh, D., Eriksson, P., Jones, A., De La Noë, J., Dupuy, E., Froidevaux, L., Livesey, N. J., Waters, J. W., and Filipiak, M. J.: Intercomparisons of trace gases profiles from the Odin/SMR and Aura/MLS limb sounders, J. Geophys. Res., 111, D21302, doi:10.1029/2006JD007305, 2006.

Beer, R.: TES on the Aura mission: scientific objectives, measurements, and analysis overview, IEEE T. Geosci. Remote, 44, 1102–1105, 2006.

Brasseur, G., Hauglustaine, D., Walters, S., Rasch, R., Müller, J.-F., Granier, C., and Tie, X.: MOZART, a global chemical transport model for ozone and related chemical tracers 1. Model description, J. Geophys. Res., 103(D21), 28265–28289, 1998.

Buchwitz, M., Khlystova, I., Bovensmann, H., and Burrows, J. P.: Three years of global carbon monoxide from SCIAMACHY: comparison with MOPITT and first results related to the detection of enhanced CO over cities, Atmos. Chem. Phys., 7, 2399–2411, 2007, http://www.atmos-chem-phys.net/7/2399/2007/.

Bowman, K. W., Rodgers, C. D., Kulawik, S. S., Worden, J., Sarkissian, E., Osterman, G., Steck, T., Ming Lou, Eldering, A., Shephard, M., Worden, H., Lampel, M., Clough, S., Brown, P., Rinsland, C., Gunson, M., and Beer, R.: Tropospheric Emission Spectrometer: Retrieval method and error analysis, IEEE T. Geosci. Remote, 44, 1297–1307, 2006.

Boynard, A., Clerbaux, C., Coheur, P.-F., Hurtmans, D., Turquety, S., George, M., Hadji-Lazaro, J., Keim, C., and Mayer-Arnek, J.: Measurements of total and tropospheric ozone from the IASI instrument: comparison with satellite and ozonesonde observations, Atmos. Chem. Phys. Discuss., in review, 2009.

Clarisse, L., Coheur, P. F., Prata, A. J., Hurtmans, D., Razavi, A., Phulpin, T., Hadji-Lazaro, J., and Clerbaux, C.: Tracking and quantifying volcanic SO_2 with IASI, the September 2007 eruption at Jebel at Tair, Atmos. Chem. Phys., 8, 7723–7734, 2008, http://www.atmos-chem-phys.net/8/7723/2008/.

Clerbaux, C., Hadji-Lazaro, J., Payan, S., Camy-Peyret, C., Wang, J., Edwards, D., and Luo, M., Retrieval of CO from nadir remote-sensing measurements in the infrared by use of four different inversion algorithms, Appl. Optics, 41(33), 7068–7078, 2002.

Clerbaux, C., Coheur, P.-F., Hurtmans, D., Barret, B., Carleer, M., Colin, R., Semeniuk, K., McConnell, J. C., Boone, C., and Bernath, P.: Carbon monoxide distribution from the ACE-FTS solar occultation measurements, Geophys. Res. Lett., 32, L16S01, doi:10.1029/2005GL022394, 2005.

Clerbaux, C., Hadji-Lazaro, J., Turquety, S., George, M., Coheur, P.-F., Hurtmans, D., Wespes, C., Herbin, H., Blumstein, D., Tournier, B., and Phulpin, T.: The IASI/MetOp mission: first observations and highlight of its potential contribution to the GMES Earth observation component, Space Research Today (COSPAR Inf. Bul.), 168, 19–24, 2007.

Clerbaux, C., George, M., Turquety, S., Walker, K. A., Barret, B., Bernath, P., Boone, C., Borsdorff, T., Cammas, J. P., Catoire, V., Coffey, M., Coheur, P.-F., Deeter, M., De Maziére, M., Drummond, J., Duchatelet, P., Dupuy, E., de Zafra, R., Eddounia, F., Edwards, D. P., Emmons, L., Funke, B., Gille, J., Griffith, D. W. T., Hannigan, J., Hase, F., Höpfner, M., Jones, N., Kagawa, A., Kasai, Y., Kramer, I., Le Flochmoën, E., Livesey, N. J., López-Puertas, M., Luo, M., Mahieu, E., Murtagh, D., Nédélec, P., Pazmino, A., Pumphrey, H., Ricaud, P., Rinsland, C. P., Robert, C., Schneider, M., Senten, C., Stiller, G., Strandberg, A., Strong, K., Sussmann, R., Thouret, V., Urban, J., and Wiacek, A.: CO measurements from the ACE-FTS satellite instrument: data analysis and validation using ground-based, airborne and spaceborne observations, Atmos. Chem. Phys., 8, 2569–2594, 2008a, http://www.atmos-chem-phys.net/8/2569/2008/.

Clerbaux, C., Edwards, D. P., Deeter, M., Emmons, L., Lamarque, J.-F., Tie, X. X., Massie, S. T., and Gille, J.: Carbon monoxide pollution from cities and urban areas observed by the Terra/MOPITT mission, Geophys. Res. Lett, 35, L03817, doi:10.1029/2007GL032300, 2008b.

Clerbaux, C., Boynard, A., Clarisse, L., George, M., Hadji-Lazaro, J., Herbin, H., Hurtmans, D., Pommier, M., Razavi, A., Turquety, S., Wespes, C., and Coheur, P.-F.: Monitoring of atmospheric composition using the thermal infrared IASI/MetOp sounder, Atmos. Chem. Phys. Discuss., 9, 8307–8339, 2009, http://www.atmos-chem-phys-discuss.net/9/8307/2009/.

Coheur, P.-F., Clarisse, L., Turquety, S., Hurtmans, D., and Clerbaux, C.: IASI measurements of reactive trace species in biomass burning plumes, Atmos. Chem. Phys. Discuss., 9, 8757-8789, 2009, http://www.atmos-chem-phys-discuss.net/9/8757/2009/.

Comer, M. M.: Retrieving Carbon Monoxide Abundances from the Atmospheric Infrared Sounder (AIRS), Ph.D. Dissertation, University of Maryland Baltimore County, USA, 2006.

Deeter, M. N., Emmons, L. K., Francis, G. L., Edwards, D. P., Gille, J. C., Warner, J. X., Khattatov, B., Ziskin, D., Lamarque, J.-F., Ho, S.-P., Yudin, V., Attié, J.-L., Packman, D., Chen, J., Mao, D., and Drummond, J. R.: Operational carbon monoxide retrieval algorithm and selected results for the MOPITT instrument, J. Geophys. Res., 108(D14), 4399, doi:10.1029/2002JD003186, 2003.

Deeter, M. N., Edwards, D. P., Gille, J. C., and Drummond, J. R.: Sensitivity of MOPITT observations to carbon monoxide in the lower troposphere, J. Geophys. Res., 112, D24306, doi:10.1029/2007JD008929, 2007.

Deeter, M. N., Edwards, D. P., Gille, J. C., and Drummond, J. R.: CO retrievals based on MOPITT near-infrared observations, J. Geophys. Res., 114, D04303, doi:10.1029/2008JD010872, 2009.

Drummond, J. R.: Novel correlation radiometer: the length-modulated radiometer, Appl. Optics, 28, 2451–2452, 1989.

Edwards, D. P., Emmons, L. K., Hauglustaine, D. A., Chu, A., Gille, J. C., Kaufman, Y. J., Pétron, G., Yurganov, L. N., Giglio, L., Deeter, M. N., Yudin, V., Ziskin, D. C., Warner, J., Lamarque, J.-F., Francis, G. L., Ho, S. P., Mao, D., Chan, J., and Drummond, J. R.: Observations of Carbon Monoxide and Aerosol From the Terra Satellite: Northern Hemisphere Variability, J. Geophys. Res., 109, D24202, doi:10.1029/2004JD0047272004, 2004.

Emmons, L. K., Deeter, M. N., Gille, J. C., et al.: Validation of Measurements of Pollution in the Troposphere (MOPITT) CO retrievals with aircraft in situ profiles, J. Geophys. Res., 109, D03309, doi:10.1029/2003JD004101, 2004.

Emmons, L. K., Pfister, G. G., Edwards, D. P., Gille, J. C., Sachse, G., Blake, D., Wofsy, S., Gerbig, C., Matross, D., and Nédélec, P.: Measurements of Pollution in the Troposphere (MOPITT) validation exercises during summer 2004 field campaigns over North America, J. Geophys. Res., 112, D12S02, doi:10.1029/2006JD007833, 2007.

Emmons, L. K., Edwards, D. P., Deeter, M. N., Gille, J. C., Campos, T., Nédélec, P., Novelli, P., and Sachse, G.: Measurements of Pollution In The Troposphere (MOPITT) validation through 2006, Atmos. Chem. Phys., 9, 1795–1803, 2009, http://www.atmos-chem-phys.net/9/1795/2009/.

Duncan, B. N. and Logan, J. A.: Model analysis of the factors regulating the trends and variability of carbon monoxide between 1988 and 1997, Atmos. Chem. Phys., 8, 7389–7403, 2008, http://www.atmos-chem-phys.net/8/7389/2008/.

Frankenberg, C., Platt, U., and Wagner, T.: Retrieval of CO from SCIAMACHY onboard ENVISAT: detection of strongly polluted areas and seasonal patterns in global CO abundances, Atmos. Chem. Phys., 5, 1639–1644, 2005, http://www.atmos-chem-phys.net/5/1639/2005/.

Funke, B., López-Puertas, M., Bermejo-Pantaleón, D., von Clarmann, T., Stiller, G. P., Höpfner, M., Grabowski, U., and Kaufmann M.: Analysis of nonlocal thermodynamic equilibrium CO 4.7 μm fundamental, isotopic, and hot band emissions measured by the Michelson Interferometer for Passive Atmospheric Sounding on Envisat, J. Geophys. Res., 112, D11305, doi:10.1029/2006JD007933, 2007.

Kulawik, S. S., Bowman, K. W., Luo, M., Rodgers, C. D., and Jourdain, L.: Impact of nonlinearity on changing the a priori of trace gas profile estimates from the Tropospheric Emission Spectrometer (TES), Atmos. Chem. Phys., 8, 3081–3092, 2008, http://www.atmos-chem-phys.net/8/3081/2008/.

Kurylo, M.: Network for the detection of stratospheric change (NDSC), in Remote sensing of atmospheric chemistry; Proceedings of the Meeting, Orlando, FL, 1-3 April, A93-31376 11–35, 168–174, 1991.

Little, A. D., Neil, D. O., Sachse, G. W., Fishman, J., and Krueger, A.: Remote sensing from geostationary orbit: GEO TROPSAT, a new concept for atmospheric remote sensing. Sensors, Systems, and Next-Generation Satellites, SPIE Proc., 3221, 480–488, 1997.

Livesey, N. J., Filipiak, M. J., Froidevaux, L., et al.: Validation of Aura Microwave Limb Sounder O_3 and CO observations in the upper troposphere and lower stratosphere, J. Geophys. Res., 113, D15S02, doi:10.1029/2007JD008805, 2008.

Logan, J., Prather, M. J., Wofsy, S. C., and McElroy, M. B.: Tropospheric chemistry: A global perspective, J. Geophys. Res., 86, 7210–7254, 1981.

Luo, M., Rinsland, C. P, Rodgers, C. D., Logan, J. A., Worden, H., Kulawik, S., Eldering, A., Goldman, A., Shephard, M. W., Gunson, M., and Lampel, M.: Comparison of carbon monoxide measurements by TES and MOPITT: Influence of a priori data and instrument characteristics on nadir atmospheric species retrievals, J. Geophys. Res., 112, D09303, doi:10.1029/2006JD007663, 2007a.

Luo, M., Rinsland, C., Fisher, B., Sachse, G., Diskin, G., Logan, J., Worden, H., Kulawik, S., Osterman, G., Eldering, A., Herman, R., and Shephard, M.: TES carbon monoxide validation with DACOM aircraft measurements during INTEX-B 2006, J. Geophys. Res., 112, D24S48, doi:10.1029/2007JD008803, 2007b.

McMillan, W. W., Barnet, C., Strow, L., Chahine, M. T., McCourt, M. L., Warner, J. X., Novelli, P. C., Korontzi, S., Maddy, E. S., and Datta, S.: Daily global maps of carbon monoxide from NASA's Atmospheric Infrared Sounder, Geophys. Res. Lett., 32, L11801, doi:10.1029/2004GL021821, 2005.

McMillan, W. W., Warner, J. X., Comer, M. M., Maddy, E., Chu, A., Sparling, L., Eloranta, E. W., Hoff, R. M., Sachse, G., Barnet, C., Razenkov, I. A., and Wolf, W.: AIRS views of transport from 12–22 July 2004 Alaskan/Canadian fires: Correlation of AIRS CO and MODIS AOD with forward trajectories and comparison of AIRS CO retrievals with DC-8 in situ measurements during INTEX-A/ICARTT, J. Geophys. Res., 113, D20301, doi:10.1029/2007JD009711, 2008.

Nedelec, P., Cammas, J.-P., Thouret, V., Athier, G., Cousin, J.-M., Legrand, C., Abonnel, C., Lecoeur, F., Cayez, G., and Marizy, C.: An improved infrared carbon monoxide analyser for routine measurements aboard commercial Airbus aircraft: technical validation and first scientific results of the MOZAIC III programme, Atmos. Chem. Phys., 3, 1551–1564, 2003, http://www.atmos-chem-phys.net/3/1551/2003/.

Nedelec, P., Thouret, V., Brioude, J., Sauvage, B., Cammas, J.-P., and Stohl, A.: Extreme CO concentrations in the upper troposphere over northeast Asia in June 2003 from the in situ MOZAIC aircraft data, Geophys. Res. Lett., 32, L14807, doi:10.1029/2005GL023141, 2005.

Neil, D. O., Gordley, L. L., Marshall, B. T., and Sachse, G. W.: Remote Sensing of Clouds and the Atmosphere V, edited by: Russell, J. E, Schaefer, K., and Lado-Bordowsky, O., SPIE Proc., 4168, 265–273, 2001.

Novelli, P., Masarie, K., and Lang, P.: Distributions and recent changes of carbon monoxide in the lower troposphere, J. Geophys. Res., 103(D15), 19015–19033, 1998.

Osterman,G., Bowman, K., Eldering, A., et al: TES Level 2 Data User's Guide, v3.1, JPL D-38042, 31 July, 2008.

Pan, L., Gille, J., Edwards, D. P., Baileys, P. L., and Rodgers, C. D.: Retrieval of carbon monoxide for the MOPITT instrument, J. Geophys. Res., 103, 32277–32290, 1998.

Pougachev, N. S. and Rinsland, C. P.: Spectroscopic study of the seasonal variation of carbon monoxide vertical distribution above Kitt Peak, J. Geophys. Res., 100, 1409–1416, 1995.

Pumphrey, H. C., Filipiak, M. J., Livesey, N. J., Schwartz, M. J., Boone, C., Walker, K. A., Bernath, P., Ricaud, P., Barret, B., Clerbaux, C., Jarnot, R. F., Manney, G. L., and Waters,

J. W.: Validation of middle-atmosphere carbon monoxide retrievals from Microwave Limb Sounder on Aura, J. Geophys. Res., 112, D24S38, doi:10.1029/2007JD008723, 2007.
Razavi, A., Clerbaux, C., Wespes, C., Clarisse, L., Hurtmans, D., Payan, S., Camy-Peyret, C., and Coheur, P. F.: Characterization of methane retrievals from the IASI space-borne sounder, Atmos. Chem. Phys. Discuss., 9, 7615–7643, 2009, http://www.atmos-chem-phys-discuss.net/9/7615/2009/.
Rinsland, C. P., Luo, M., Logan, J. A., Beer, R., Worden, H., Kulawik, S. S., Rider, D., Osterman, G., Gunson, M., Eldering, A., Goldman, A., Shephard, M., Clough, S. A., Rodgers, C., Lampel, M., and Chiou, L.: Nadir measurements of carbon monoxide (CO) distributions by the tropospheric emission spectrometer instrument onboard the Aura spacecraft: Overview of analysis approach and examples of initial results, Geophys. Res. Lett., 33, L22806, doi:10.1029/2006GL027000, 2006.
Rinsland, C. P., Luo, M., Shephard, M. W., Clerbaux, C., Boone, C. D., Bernath, P. F., Chiou, L., and Coheur, P. F.: Tropospheric emission spectrometer (TES) and atmospheric chemistry experiment (ACE) measurements of tropospheric chemistry in tropical southeast Asia during a moderate El Niño in 2006, J. Quant. Spectrosc. Ra., 109, 1931–1942, doi:10.1016/j.jqsrt.2007.12.020, 2008.
Rodgers, C. D.: Inverse methods for atmospheric sounding : theory and practice, Ser. Atmos. Oceanic Planet. Phys., 2, World Sci., edited by: Hackensack, N. J., 2000.
Schluessel, P., Hultberg, T. H., Phillips, P. L. T., August, T., and Calbet, X.: The operational IASI Level 2 processor, Adv. Space Res., 36, 982–988, 2005.
Susskind, J., Barnet, C. D., and Blaisdell, J. M.: Retrieval of atmospheric and surface parameters form AIRS/AMSU/HSB data in the presence of clouds, IEEE T. Geosci. Remote, 41, 390–409, 2003.
Turquety, S., Hadji-Lazaro, J., Clerbaux, C., Hauglustaine, D. A., Clough, S. A., Cassé, V., Schlüssel, P., and Mégie, G.: Operational trace gas retrieval algorithm for the Infrared Atmospheric Sounding Interferometer, J. Geophys. Res., 109, D21301, doi:10.1029/2004JD004821, 2004.
Turquety, S., Clerbaux, C., Law, K., Coheur, P.-F., Cozic, A., Szopa, S., Hauglustaine, D. A., Hadji-Lazaro, J., Gloudemans, A. M. S., Schrijver, H., Boone, C. D., Bernath, P. F., and Edwards, D. P.: CO emission and export from Asia: an analysis combining complementary satellite measurements (MOPITT, SCIAMACHY and ACE-FTS) with global modeling, Atmos. Chem. Phys. Discuss., 8, 1709–1755, 2008,

http://www.atmos-chem-phys-discuss.net/8/1709/2008/.
Turquety, S., Hurtmans, D., Hadji-Lazaro, J., Coheur, P.-F., Clerbaux, C., Josset, D., and Tsamalis, C.: Tracking the emission and transport of pollution from wildfires using the IASI CO retrievals: analysis of the summer 2007 Greek fires, Atmos. Chem. Phys. Discuss., 9, 7413–7455, 2009, http://www.atmos-chem-phys-discuss.net/9/7413/2009/.
Velazco, V., Wood, S. W., Sinnhuber, M., Kramer, I., Jones, N. B., Kasai, Y., Notholt, J., Warneke, T., Blumenstock, T., Hase, F., Murcray, F. J., and Schrems, O.: Annual variation of strato-mesospheric carbon monoxide measured by ground-based Fourier transform infrared spectrometry, Atmos. Chem. Phys., 7, 1305–1312, 2007, http://www.atmos-chem-phys.net/7/1305/2007/.
Warner, J., McCourt Comer, M., Barnet, C. D., McMillan, W. W., Wolf, W., Maddy, E., and Sachse, G.: A comparison of satellite tropospheric carbon monoxide measurements from AIRS and MOPITT during INTEX-A, J. Geophys. Res., 112, D12S17, doi:10.1029/2006JD007925, 2007.
Wespes, C., Hurtmans, D., Clerbaux, C., Santee, M. L., Martin, R. V., and Coheur, P. F.: Global distributions of nitric acid from IASI/MetOP measurements, Atmos. Chem. Phys. Discuss., 9, 8035–8069, 2009, http://www.atmos-chem-phys-discuss.net/9/8035/2009/.
Worden, H., Beer, R., Bowman, K. W., Fisher, B., Luo, M., Rider, D., Sarkissian, E., Tremblay, D., and Zong, J.: TES Level 1 Algorithms: Interferogram Processing, Geolocation, Radiometric, and Spectral Calibration, IEEE T. Geosci. Remote, 44, 1288–1296, 2006.
Yurganov, L. N., Blumenstock, T., Grechko, E. I., Hase, F., Hyer, E. J., Kasischke, E. S., Koike, M., Kondo, Y., Kramer, I., Leung, F.-Y., Mahieu, E., Mellqvist, J., Notholt, J., Novelli, P. C., Rinsland, C. P., Scheel, H. E., Schulz, A., Strandberg, A., Sussmann, R., Tanimoto, H., Velazco, V., Zander, R., and Zhao, Y.: A quantitative assessment of the 1998 carbon monoxide emission anomaly in the Northern Hemisphere based on total column and surface concentration measurements, J. Geophys. Res., 109, D15305, doi:10.1029/2004JD004559, 2004.
Yurganov, L. N., Duchatelet, P., Dzhola, A. V., Edwards, D. P., Hase, F., Kramer, I., Mahieu, E., Mellqvist, J., Notholt, J., Novelli, P. C., Rockmann, A., Scheel, H. E., Schneider, M., Schulz, A., Strandberg, A., Sussmann, R., Tanimoto, H., Velazco, V., Drummond, J. R., and Gille, J. C.: Increased Northern Hemispheric carbon monoxide burden in the troposphere in 2002 and 2003 detected from the ground and from space, Atmos. Chem. Phys., 5, 563–573, 2005,

http://www.atmos-chem-phys.net/5/563/2005/.
Yurganov, L. N., McMillan, W. W., Dzhola, A. V., Grechko, E. I., Jones, N. B., and van der Werf, G. R.: Global AIRS and MOPITT CO measurements: Validation, comparison, and links to biomass burning variations and carbon cycle, J. Geophys. Res., 113, D09301, doi:10.1029/2007JD009229, 2008.
Zander, R., Mahieu, E., Demoulin, P., Duchatelet, P., Roland, R., Servais, C., De Mazière, M., Reimann, S., and Rinsland, C. P.: Our changing atmosphere: Evidence based on long-term infrared solar observations at the Jungfraujoch since 1950, Sci. Total Environ., 391, 184–195, doi:10.1016/j.scitotenv.2007.10.018, 2008.

Table 1. Description of current missions and instruments that measure tropospheric CO from nadir TIR radiances. All missions are on polar sun-synchronous orbiting platforms. Specifications are given for the CO thermal IR spectral range only, and for the nadir geometry.

Mission/Plate-form Agency Launch date Data (L1) availability	Plate-form altitude Equator crossing time, descending/ascending orbit Instrument type	Spectral coverage (cm^{-1}) Pixel size, Spatial coverage Spectral resolution Radiometric precision for CO lines	References
IASI/MetOp EUMETSAT/CNES October 2006 May 2007	817 km 09:30, descending FTS, 8461 channels, OPD 2 cm	645 to 2760 12 km diam×4 pixels, swath 2200 km 0.5 cm^{-1} (apodized) 0.25 K (NeDT@280K)	Schluessel et al., 2005 Turquety et al., 2004 Clerbaux et al., 2007, 2009
MOPITT/TERRA NASA (EOS) December 1999 March 2000	705 km 10:30, descending Gas correlation radiometer ; 3 bands, 8 channels	2140–2192, 4265–4305 22×22 km, swath 640 km 0.04 cm^{-1} (effective) 0.05 K (NeDT@280K)	Drummond, 1989 Edwards et al., 2004 Deeter et al., 2003, 2007
AIRS/AQUA NASA (EOS) May 2002 August 2002	705 km 13:30, ascending Grating spectrometer, 2378 channels, resolving power $\lambda/\Delta\lambda$ =1200	650–1136, 2116–1613, 2170–2674 13.5×13.5 km×9 pixels, swath 1650 km ~1.8 cm^{-1} (2170–2200 cm^{-1}) 0.14 K (NeDT@280K)	McMillan et al., 2005, 2008 Aumann et al., 2003
TES/AURA NASA (EOS) July 2004 August 2004	705 km 13:45, ascending FTS, 40540 channels, OPD 8.45 cm	652–919(2B1), 923–1160(1B2), 1090–1339(2A1) and 1891–2251(1A1) 5.3×8.3 km×16 pixels, no swath 0.10 cm^{-1} (apodized) 1.5 K (NeDT @300K)	Beer et al., 2006 Bowman et al., 2006 Rinsland et al., 2006 Luo et al., 2007a and b Worden et al., 2006

ACPD
9, 9793–9822, 2009

Table 2. Correlation coefficients corresponding to Fig. 6.

	MOPITT	AIRS	TES
Global	Corr. coeff.=0.82 Slope=0.93 Intercept=−0.05	Corr. coeff.=0.91 Slope=1.68 Intercept=-1.3	Corr. coeff.=0.83 Slope=0.85 Intercept=0.37
Lat [45°; 90°]	Corr. coeff.=0.7 Slope=0.5 Intercept=0.83	Corr. coeff.=0.88 Slope=1.11 Intercept=−0.2	Corr. coeff.=0.55 Slope=0.38 Intercept=1.19
Lat [15°; 45°]	Corr. coeff.=0.83 Slope=0.96 Intercept=0.01	Corr. coeff.=0.79 Slope=1.28 Intercept=−0.5	Corr. coeff.=0.73 Slope=0.83 Intercept=0.46
Lat [−15°; 15°]	Corr. coeff.=0.93 Slope=0.89 Intercept=0.13	Corr. coeff.=0.94 Slope=1.75 Intercept=−1.42	Corr. coeff.=0.87 Slope=0.89 Intercept=0.32
Lat [−45°; −15°]	Corr. coeff.=0.73 Slope=0.77 Intercept=0.14	Corr. coeff.=0.86 Slope=1.27 Intercept=−0.67	Corr. coeff.=0.75 Slope=0.65 Intercept=0.56

ACPD
9, 9793–9822, 2009

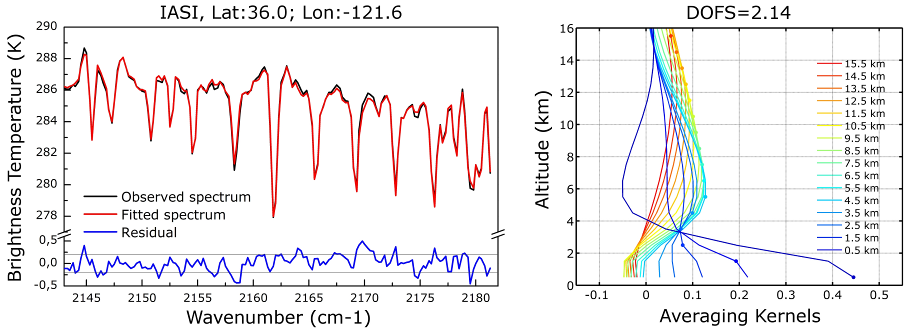

Fig. 1. Left panel: spectral range used for the FORLI-CO retrieval. The spectrum (in brightness temperature units) was recorded around 09:30 local time, on 1 August 2008, close to Los Angeles (USA). The residual difference (blue) between the measured spectrum (black) and the calculated spectrum (red) is within the IASI radiometric noise (0.2 K) as indicated by the grey horizontal lines. Right panel: FORLI-CO averaging kernels functions, for the same observation, for different merged vertical layers.

ACPD
9, 9793–9822, 2009

Carbon monoxide distributions from the IASI/METOP mission

M. George et al.

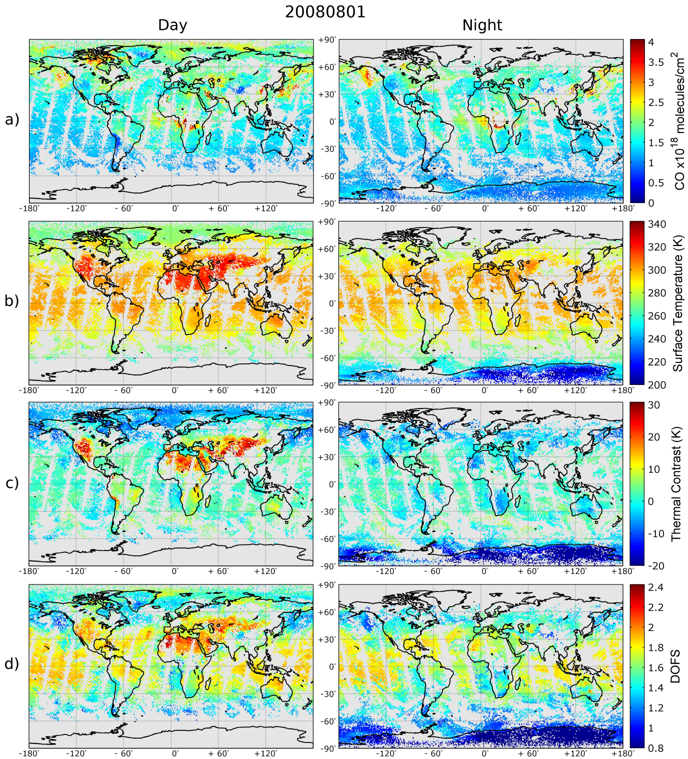

Fig. 2. IASI global distributions on 1 August 2008, for daytime (left) and night time (right). Cloud free observations are binned on a 0.5°×0.5° grid. **(a)** CO total column distribution as retrieved by FORLI-CO. **(b)** Surface temperature (available from Eumetsat). **(c)** Thermal contrast as calculated from the difference between surface temperature and the temperature of the first available level of temperature profile. **(d)** Degrees of freedom of the signal (DOFS) as calculated from the averaging kernel matrices.

ACPD

9, 9793–9822, 2009

Carbon monoxide distributions from the IASI/METOP mission

M. George et al.

ACPD
9, 9793–9822, 2009

Carbon monoxide distributions from the IASI/METOP mission

M. George et al.

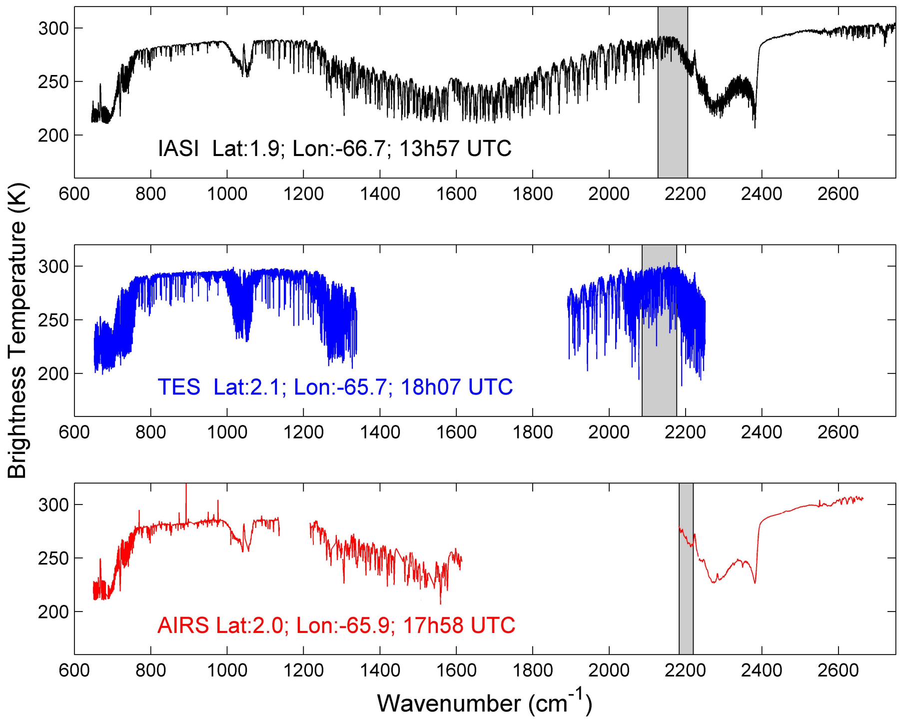

Fig. 3. IASI, TES and AIRS radiance spectra (in brightness temperature) around Northern Brazil, on 1 August 2008. The spectral range used for the CO retrieval are highlighted in grey.

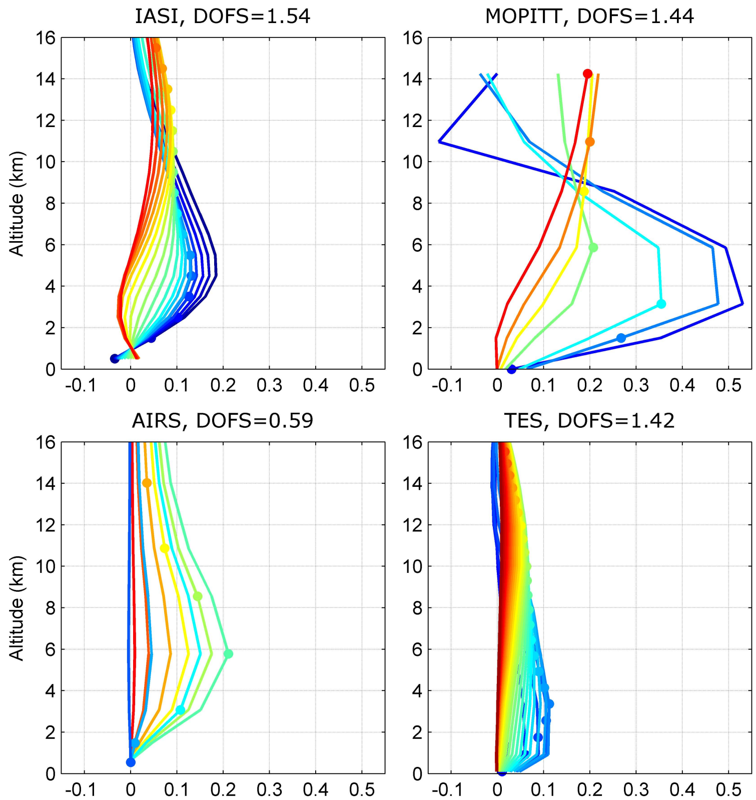

Fig. 4. Comparison of IASI, MOPITT, AIRS and TES averaging kernels and DOFS. IASI, AIRS and TES averaging kernels correspond to the inversion of the spectra provided in Fig. 3. The MOPITT averaging kernels are chosen the same day at about the same localisation. Each coloured line corresponds to the altitude indicated by coloured dot. Averaging kernels depend on vertical grid spacing, which is different for each instrument.

ACPD

9, 9793–9822, 2009

Carbon monoxide distributions from the IASI/METOP mission

M. George et al.

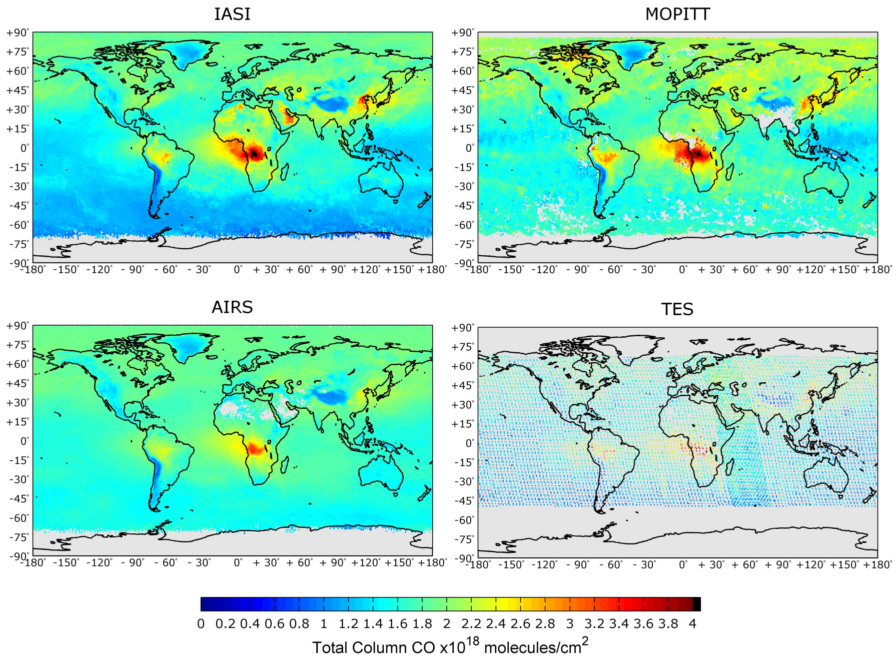

Fig. 5. Averaged IASI, MOPITT, AIRS and TES CO total column distributions, binned on a $1^\circ \times 1^\circ$ grid, for August 2008. All observations are for day-time, and were cloud-filtered following the recommendation provided by each retrieval team. There are more TES data between 30° W and 90° W because data are recorded every 2 days for 26 h.

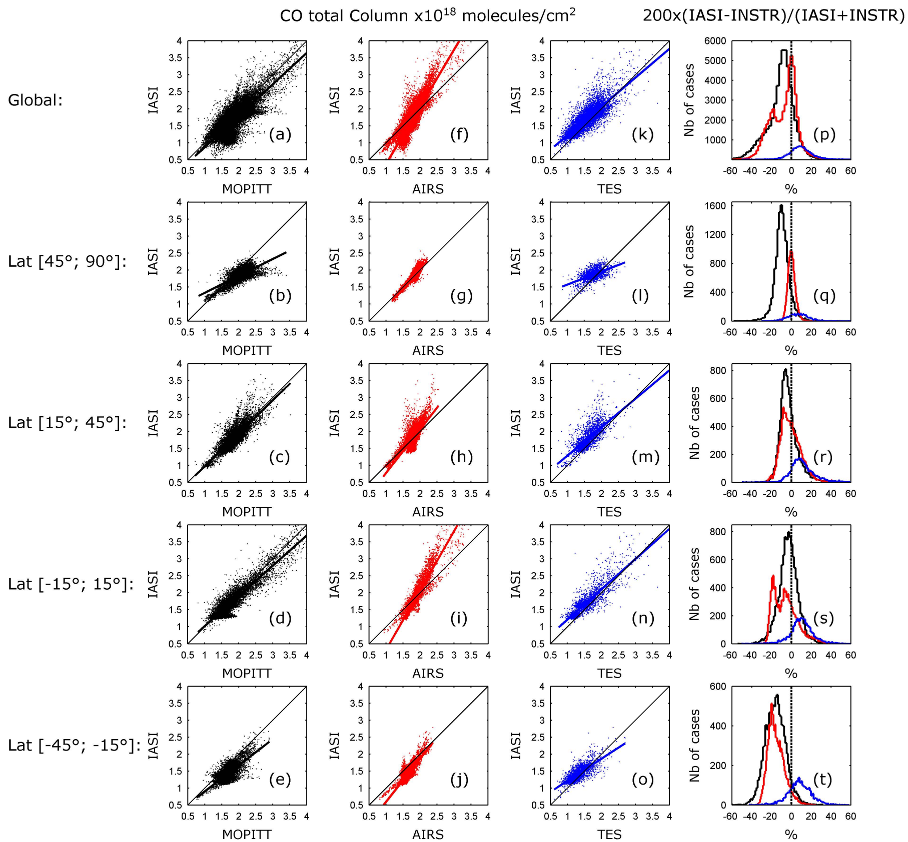

Fig. 6. Scatter plots between IASI and MOPITT, AIRS, TES, for different latitudes bands (see correlation coefficients in Table 2) and histograms of the differences in percent (200×IASI-INSTR/IASI+INSTR).

ACPD
9, 9793–9822, 2009

Title Page
Abstract Introduction
Conclusions References
Tables Figures
◄ ►
Back Close
Full Screen / Esc
Printer-friendly Version
Interactive Discussion